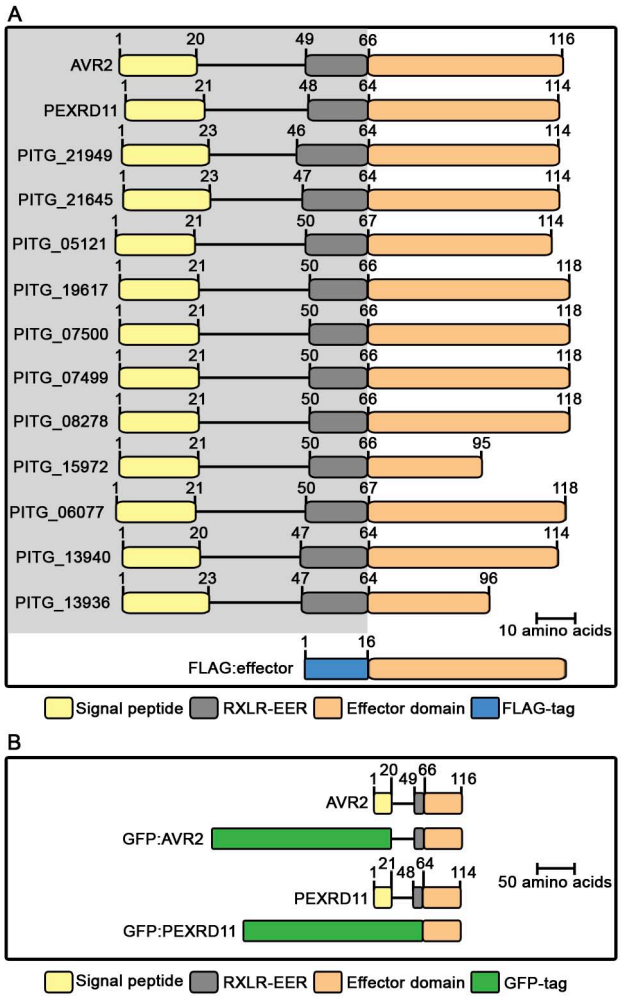

Supplemental Figure 1. Schematic representation of AVR2 family fusion constructs used in co-IPs. **(A)** The C-terminal effector domains (orange box) of twelve of the AVR2 family members were fused to the FLAG epitope tag at the N-terminus in place of the signal peptide and RXLR domain (highlighted in grey). For PEXRD11, the FLAG epitope tag was added in place of the signal peptide region alone. **(B)** The mature AVR2 protein (excluding the signal peptide region) and PEXRD11 effector domain were fused to the green fluorescent protein (GFP) at the N-terminus to create the fusion proteins GFP:AVR2 and GFP:PEXRD11, respectively. Numbers indicate position of the amino acid residues.

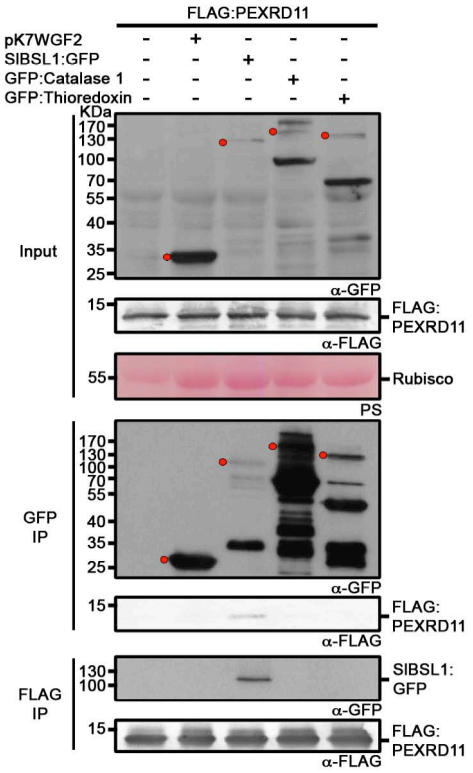

Supplemental Figure 2. Immunoblots showing that *P. infestans* PEXRD11 specifically associates with Sl-BSL1 *in planta*. FLAG:PEXRD11 was transiently expressed alone, with pK7WGF2 or with GFP-tagged putative target proteins in *N. benthamiana*. Immunoprecipitates obtained with anti-FLAG or anti-GFP antiserum and total protein extracts were immunoblotted with appropriate antisera. The expected sizes of the GFP fusion proteins are indicated by red dots in the crude extracts and GFP co-IP probed with anti-GFP antibody. PS, Ponceau stain.

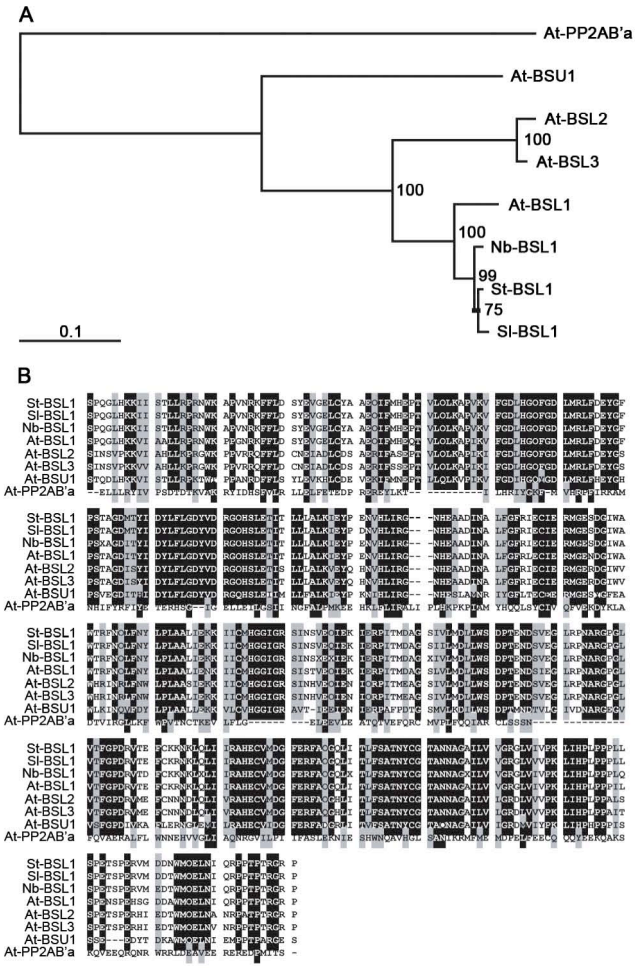

Supplemental Figure 3. Sequence analysis confirms that BSL1 from *Solanum tubersosum* (potato), *Solanum lycopersicum* (tomato) and *Nicotiana benthamiana* are orthologs of *A. thaliana* BSL1. **(A)** Phylogenetic analysis reveals that from the *Arabidopsis* BSU family, At-BSL1 is the closest ortholog of the potato, tomato and *N. benthamiana* BSL1 amino acid sequences. TOPALi v2.5 (Milne et al. 2009) was used to draw a Neighbour joining tree with a 500 bootstrap, midpoint rooted, with sequences of the C-terminal phosphatase domains of each protein **(B)**. The tree was re-rooted in FigTree v1.3.1 (http://tree.bio.ed.ac.uk/software/figtree/) to the outlier AtPP2AB'a (At3g09880). AtPP2AB'a (At3g09880), which is a component of the brassinosteroid pathway (Tang et al., 2011) was included as an outlier as the BSL phosphatases are members of the PP2A family. The tree was visualized using treeview (http://taxonomy.zoology.gla.ac.uk/rod/treeview.html). **(B)** Sequence alignment of *Arabidopsis* BSU family and potato, *N. benthamiana* and tomato BSL1 phosphatase domain-containing regions used for the Neighbour joining tree in **(A)**. Sequences were aligned using ClustalW from 522 to 869 amino acids for the BSL1 proteins, 658 to 1005 amino acids for At-BSL2, 647 to 994 for At-BSL3, 467 to 810 for At-BSU1 and 185 to 495 amino acids for At-PP2AB'a proteins. The graphic view was generated in BioEdit and imported into TOPALi v2.5 for phylogenetic analysis.

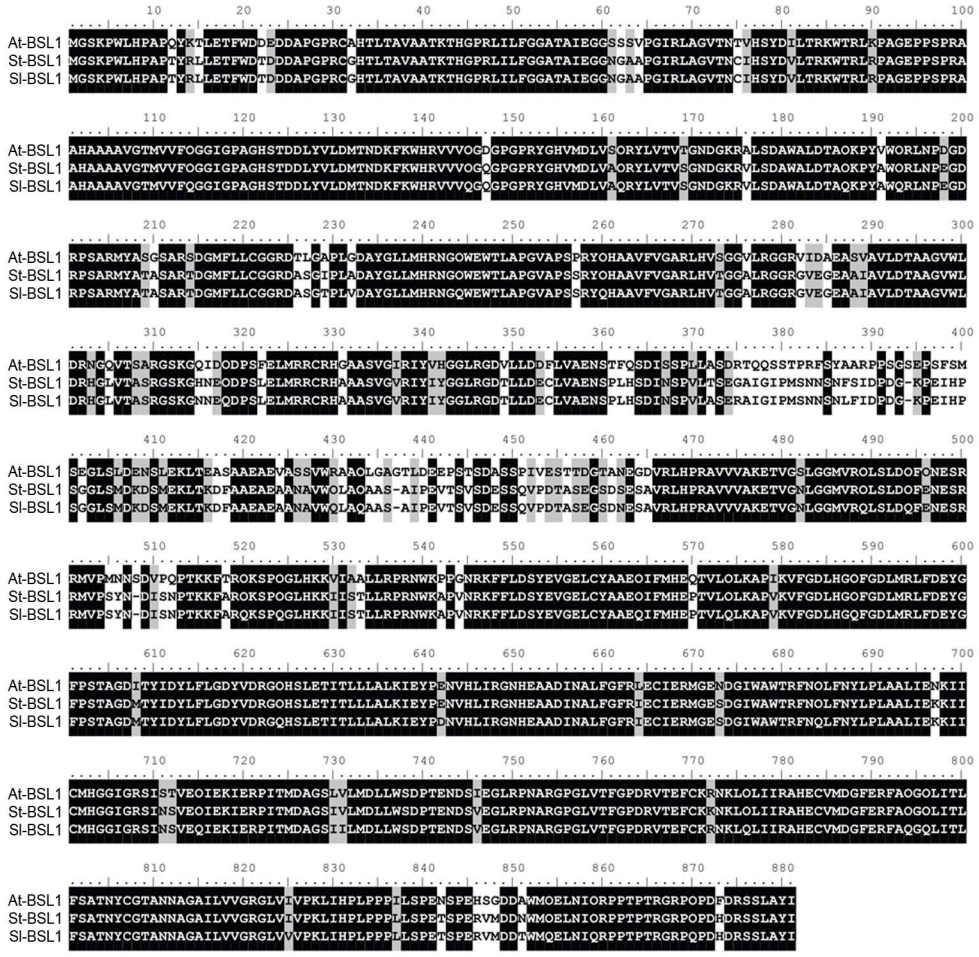

Supplemental Figure 4. *Arabidopsis*, *Solanum tubersosum* (potato) and *Solanum lycopersicum* (tomato) BSL1 full-length amino acid sequences are highly conserved. Sequences were aligned using ClustalW and the graphic view generated in BioEdit. The N-terminal kelch-repeat domain covers amino acids 18-369 and the phosphatase domain is from 520-869 amino acids.

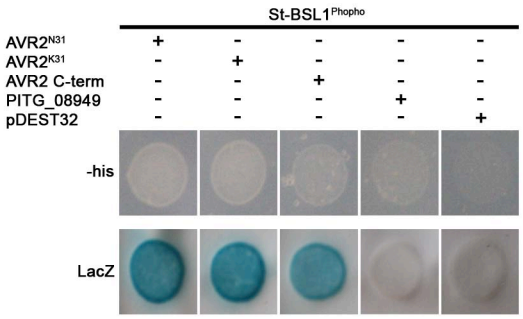

Supplemental Figure 5. Y2H analysis illustrating that *P. infestans* AVR2^{K31}, AVR2^{N31} and the C-terminal effector domain of AVR2 (amino acids 66-116) interact with the phosphatase domain (amino acids 520-881) of potato BSL1 (St-BSL1) *in vivo*. Both LacZ (giving blue colour) and His3 (providing growth on medium lacking histidine [-his]) reporter genes were activated. Empty vector (pDEST32) and the effector PITG_08949 (Gilroy et al., 2011) were used as negative controls.

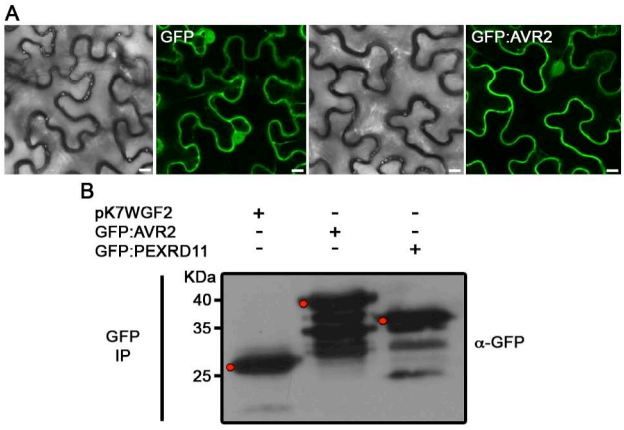

Supplemental Figure 6. Localization and stability of *P. infestans* AVR2 *in planta*. **(A)** GFP:AVR2 localizes at the cell periphery and weakly in the cytoplasm and nucleus. **(B)** GFP:AVR2 and GFP:PEXRD11 fusion proteins were partially cleaved when expressed *in planta*. pK7WGF2, GFP:AVR2 and GFP:PEXRD11 were transiently expressed in *N. benthamiana*. Immunoprecipitates obtained with anti-GFP antiserum were immunoblotted with appropriate antisera. The expected sizes of the GFP fusion proteins are indicated by red dots. Scale bars represent 10 μm.

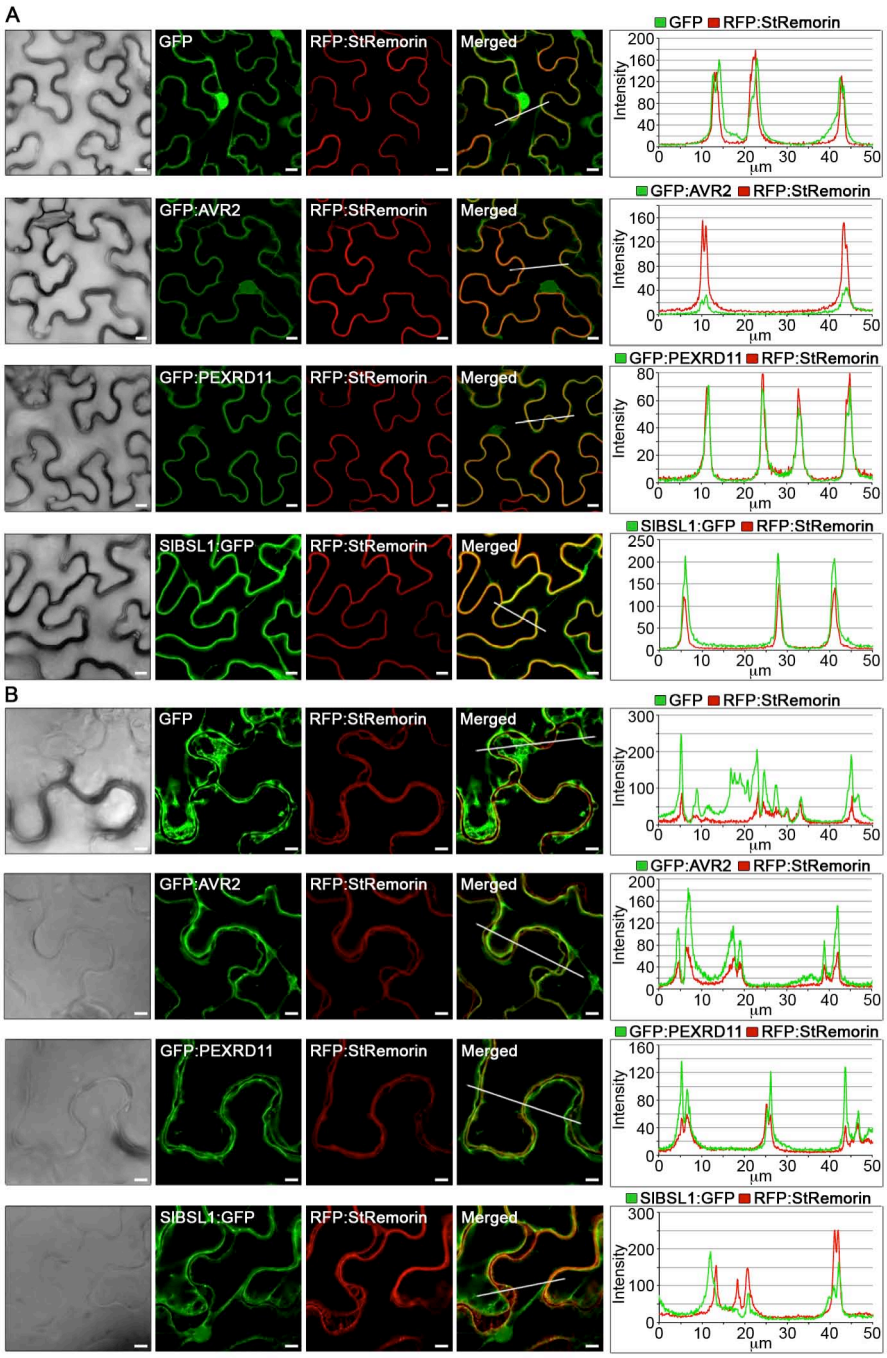

Supplemental Figure 7. *P. infestans* AVR2 and PEXRD11 co-localize with the plasma membrane-associated protein Remorin *in planta*. **(A)** GFP:AVR2, GFP:PEXRD11 and, to a large extent, SlBSL1:GFP co-localized with RFP:StRemorin at the plasma membrane when co-expressed transiently in *N. benthamiana*. **(B)** Following salt-induced plasmolysis, GFP:AVR2 and GFP:PEXRD11 clearly co-localized with RFP:StRemorin, as illustrated by overlapping peaks in the fluorescence intensity graphs. However, SlBSL1:GFP only partially co-localized with RFP:StRemorin following salt-induced plasmolysis. Pictures taken 3 dpi, scale bars represent 10 **(A)** or 5 **(B)** µm.

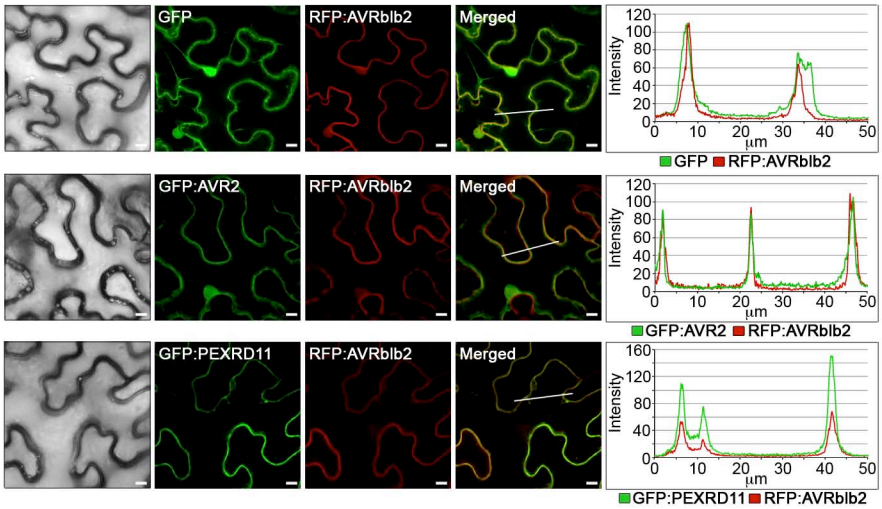

Supplemental Figure 8. *P. infestans* AVR2 and PEXRD11 co-localize with the *P. infestans* plasma membrane-associated effector AVRblb2 in planta. GFP:AVR2 and GFP:PEXRD11 co-localized with RFP:AVRblb2 in *N. benthamiana*, as illustrated by overlapping peaks in the fluorescence intensity graphs. Pictures taken 4 dpi, scale bars represent 10 µm.

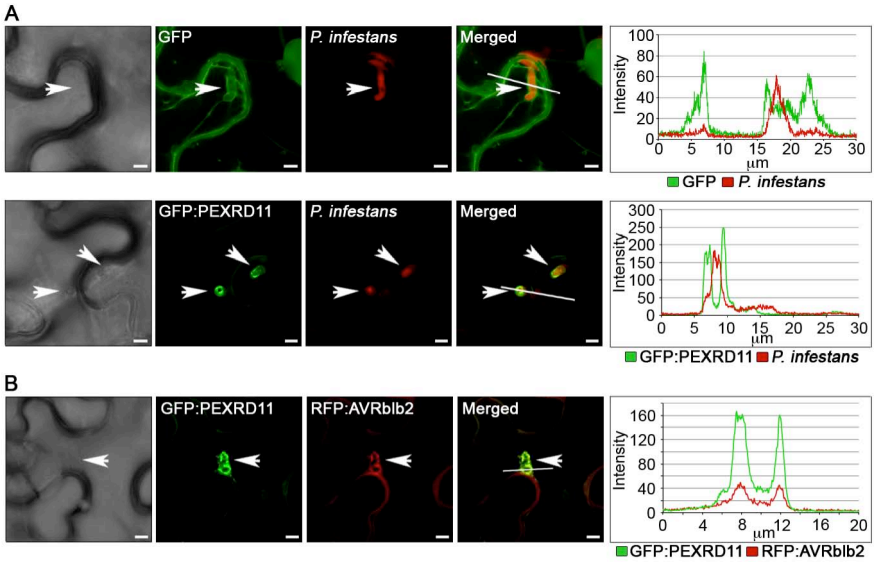

Supplemental Figure 9. *P. infestans* PEXRD11 accumulates around haustoria and co-localizes with the perihaustorial-localized effector AVRblb2 *in planta*. **(A)** *P. infestans* (red) infected *N. benthamiana* cells preferentially accumulated GFP:PEXRD11 (green) around haustoria (arrowheads), when compared to the expression of GFP alone, which maintained high levels of fluorescence throughout the cell. **(B)** *P. infestans* infected cells accumulated GFP:PEXRD11 and RFP:AVRblb2 preferentially at sites of haustorial penetration (arrowheads). Pictures were taken at 4 dpi, scale bars represent 5 µm.

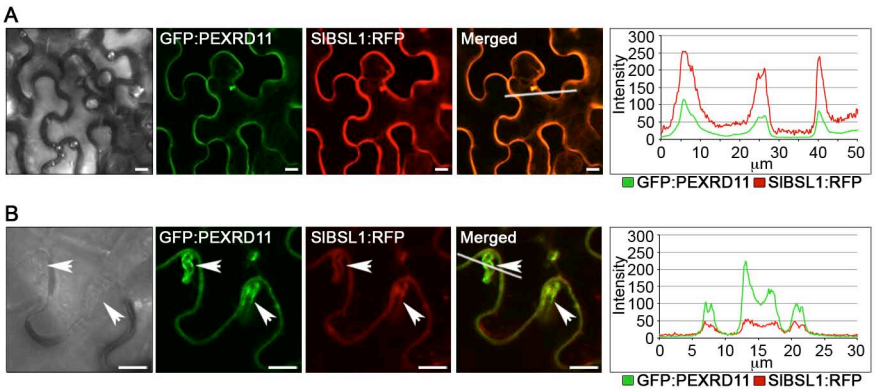

Supplemental Figure 10. Tomato BSL1 and *P. infestans* PEXRD11 colocalize *in planta* and accumulate around haustoria. **(A)** Transient expression of GFP:PEXRD11 and SlBSL1:RFP fusion proteins revealed similar patterns of localization for the two markers, accumulating at the cell periphery and within the cytoplasm. **(B)** *P. infestans* infected cells accumulated GFP:PEXRD11 and SlBSL1:RFP at sites of haustorial penetration (arrowheads). Scale bars represent 10 µm.

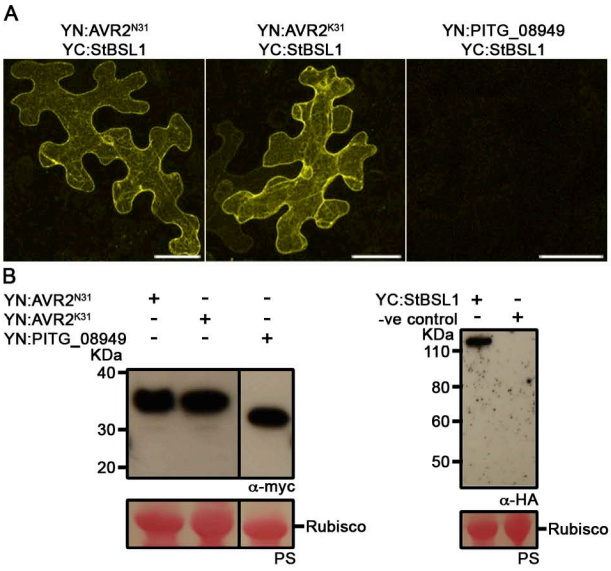

Supplemental Figure 11. AVR2 is in close proximity to St-BSL1 at the cell periphery and within the cytosol. **(A)** Bimolecular fluorescence complementation (BiFC) illustrated an association between YN:AVR2^{N31} or YN:AVR2^{K31} and YC:StBSL1 at the plasma membrane (smooth cell surface fluorescence) and in the cytosol, but not within nuclei. The N-terminus (YN) of YFP was fused to full length AVR2^{N31}, AVR2^{K31}, or PITG_08949 (excluding the signal peptide region) and co-expressed with St-BSL1 fused to the C-terminal half of YFP (YC). Images are projected stacks of 50 confocal images covering a depth of 43 µm. Scale bars represent 50 µm. **(B)** Immunoblots showing that YN:AVR2, YN:PITG_08949 and YC:StBSL1 fusion proteins were stable *in planta*. Immunoblots were probed with GFP antisera. PS, Ponceau stain.

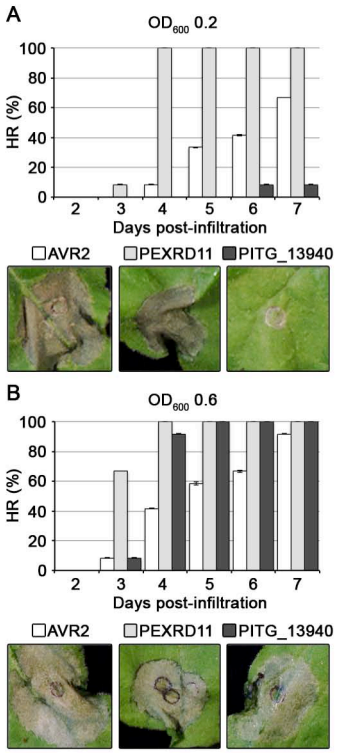

Supplemental Figure 12. PITG_13940 activates R2-mediated hypersensitivity (HR). AVR2, PEXRD11 or PITG_13940 were co-expressed with R2 in *N. benthamiana* using agroinfiltration and a final OD_{600} of 0.2 **(A)** or 0.6 **(B)**. HR (%) indicates the percentage of infiltration sites showing a confluent zone of cell death. Error bars represent +/- SE. Graphs represent 2 biological replicates, of 6 inoculation sites for each combination. Pictures were taken 4 days post-infiltration.

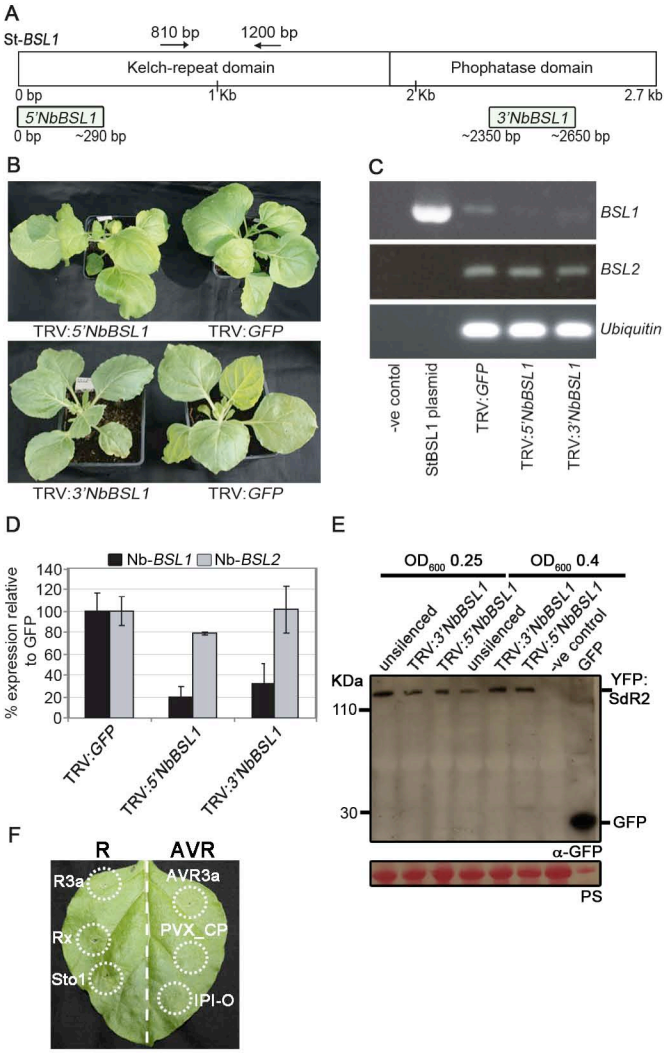

Supplemental Figure 13. Virus-induced gene silencing (VIGS) of *BSL1* in *N. benthamiana*. **(A)** Schematic representation of St-*BSL1*, which was used as a reference to design the locations of fragments of Nb-*BSL1* that were cloned into the TRV-based silencing construct (green boxes). Arrows indicate the locations of primer-annealing sites for amplification of a fragment of Nb-*BSL1* used to confirm silencing by RT-PCR. **(B)** *BSL1*-silenced plants did not show any marked phenotypic alterations when compared to TRV:*GFP* control plants. Using semi-quantitative **(C)** and quantitative **(D)** RT-PCR, VIGS of Nb-*BSL1* with either 3' or 5' silencing constructs resulted in a specific reduction in expression of Nb-*BSL1* in *N. benthamiana* compared to the expression of a second *BSU*-like gene, Nb-*BSL2*. **(E)** Immunoblots showing that R2 is stable in the *BSL1* VIGS plants. Total protein extracts were immunoblotted with an anti-GFP antibody. PS, Ponceau stain. **(F)** Expression of either effectors (AVR3a, PVX-CP, ipiO1) or corresponding resistance proteins (R3a, Rx, Sto1) alone in *BSL1*-silenced plants did not induce cell death.

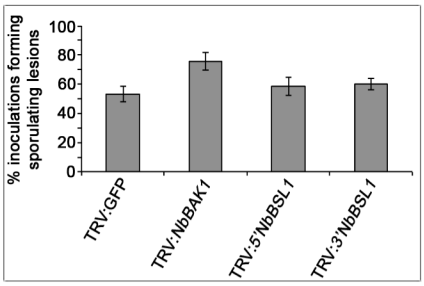

Supplemental Figure 14. VIGS of *BSL1* in *N. benthamiana* did not affect colonisation by *P. infestans*. Percentage of inoculation sites showing sporulation 6 days post-inoculation on plants expressing TRV:*GFP*, TRV:*NbBAK1*, TRV:*5'NbBSL1* or TRV:*3'NbBSL1*. There was no statistically significant increase in susceptibility to *P. infestans* for plants expressing TRV:*GFP*, TRV:*5'NbBSL1* or TRV:*3'NbBSL1*, when compared to *BAK1*-silenced plants which display increased susceptibility to *P. infestans* (Chaparro-Garcia *et al*., 2011). Statistical analysis was performed using the Holm-Sidak method in a one-way ANOVA on the Sigmaplot statistical software package. *P. infestans* colonisation was significantly different only on TRV:*NbBAK1* plants. The graph represents 7 biological replicates, each using 4 plants for each construct, 3 leaves inoculated per plant (84 inoculation sites per construct).

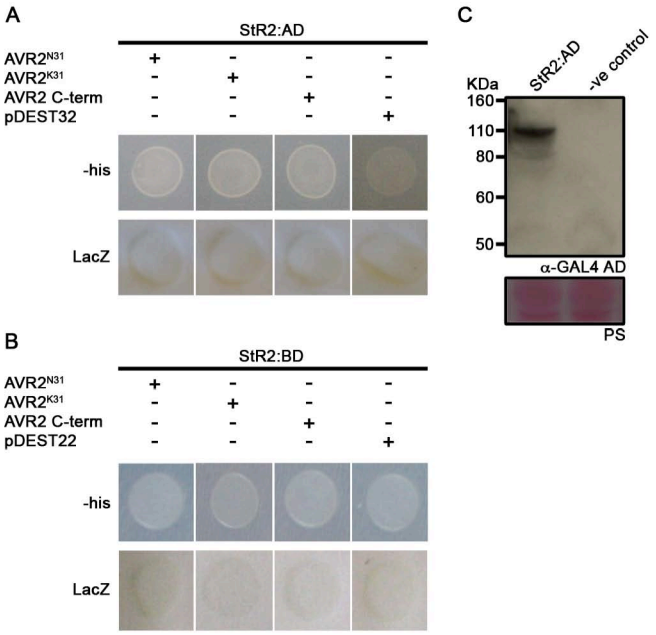

Supplemental Figure 15. Y2H analysis failed to demonstrate a direct interaction between AVR2 and R2. **(A, B)** Y2H analysis illustrating that AVR2^{K31}, AVR2^{N31}, and the C-terminal effector domain of AVR2 (amino acids 66-116) do not interact with potato R2 in vivo. Both LacZ (giving blue colour) and His3 (providing growth on synthetic-complete (-leu, -trp) medium lacking histidine [-his]) reporter genes were not activated. Empty vector (pDEST32 or pDEST22 as indicated) was used as a negative control. AVR2 and R2 were fused to both the activation and binding domains of α-GAL4 **(B)** Immunoblots showing that St-R2 was stable when expressed in yeast cells. Total protein extracts were immunoblotted with an antibody that targets the GAL4 activation domain (α-GAL4 AD). PS, Ponceau stain.

Supplemental Table 1. Plant proteins that specifically associated with AVR2 family effectors after co-immunoprecipitation as identified by mass spectrometry. Eight AVR2 homologs formed protein complexes detectable by LC-MS/MS.

Annotation for plant proteins identified in association with effector*	GenBank Accession number	Number of unique peptides matched to plant proteins in each effector co-immunoprecipitation experiment†								
		FLAG: RFP	PITG_ 21645	PITG_ 13940	PEX RD11	PITG_ 07500	PITG_ 07499	PITG_ 08278	PITG_ 06077	PITG_ 21949
Catalase 1	JQ886090	0	4	2	3	3	5	3	1	4
Serine/threonine-protein phosphatase BSL1 (BSU1-like protein 1)	JQ886089	0	7	0	8	0	0	0	0	0
Thioredoxin peroxidase	JQ886091	0	2	4	2	5	4	2	3	0

*Annotations were part of the sequences downloaded from source

†Peptide spectrum matching results were from Mascot (Matrix Science) searches and only those matching with probability score >95% are shown; Numbers reflect the number of unique peptides matched per protein; FLAG:RFP was used as negative control. Matching peptide sequences and other detail information are reported in Table S2.

Supplemental Table 2. Details of primers used in this study.

Primer name	Sequence (5'>3')
5AVR2	CACCATGCTGCATGCAGCTCCAGGTGCCAAG
3AVR2	TTAACTCCTCTTGTCACCCTTAATTTTCAAATG
5RD11	CACCACCGGAGGCTTACTGGATAAGA
3RD11	CTATTTGTACCCCTGTCCCTTTG
5BSL1	CACCATGGGTTCAAAGCCATGGC
3BSL1	AATATAGGCAAGTGAGCTCCGG
5Cat1	CACCGATCCATACAAGTATCGTCCGTCA
3Cat1	TCATATGCTTGGTCTCACATTAAG
5Thper	CACCGCTTGCTCTGCTTCTTCTACA
3Thper	TCATATGGATGCAAAGTATTC
3BSL1_kel	TGATTTCTGCCTTGCGAAC
5BSL1_phos	CACCATGCCTCAAGGATTGCATAAAAAGATC
FStrem13	AAAAAGCAGGCTTCATGGCAGAATTGGAAGCT
RStrem13	AGAAAGCTGGGTCTCAAAATATTCCAAGGAT
5Nterm_R2	CACC GCTGATGCCTTTCTATCATTTG
3Nterm_R2	TCACAACATATAATTCCGCTTCAAC
5StBSL1-1	AAAGCAGGCTTCATGGGTTCAAAGCCATGG
3StBSL1-1	GAAAGCTGGGTATTAAATATAGGCAAGTGAGCT
5StBSL1-2	GGGGACAAGTTTGTACAAAAAAGCAGGCT
3StBSL1-2	GGGGACCACTTTGTACAAGAAAGCTGGG
5StBSL-CT	AAAGCAGGCTTCATGGTGAGGCAATTGTCA
5BSL1-290	TAAAGAATTCATGGGTTCAAAGCCAT
3BSL1-290	TTTTGTTAACTCACCGGCAGGTCTAAGT
5BSL1-300	ATTTGAATTCTGCATTGAGAGAATCCCACA
3BSL1-300	TTTAGTTAACACGATCAGGCCCAAATGTTA
5BSL1-RT	AGGCGATAGACCGTCAGCTA
3BSL1-RT	CGCATAAGCTCCAAAGAAGG
5BSL2-RT	TGCACGCAGTTATGGAGAAG
3BSL2-RT	AACCAGCAGAATTCCCTTCA

Supplemental References:

Chaparro-Garcia, A., Wilkinson, R.C., Gimenez-Ibanez, S., Findlay, K., Coffey, M.D., Zipfel, C., Rathjen, J.P., Kamoun, S., and Schornack, S. (2011). The receptor-like kinase SERK3/BAK1 is required for basal resistance against the late blight pathogen phytophthora infestans in Nicotiana benthamiana. PLoS One **6,** e16608.

Gilroy, E.M., Breen, S., Whisson, S.C., Squires, J., Hein, I., Kaczmarek, M., Turnbull, D., Boevink, P.C., Lokossou, A., Cano, L.M., et al. (2011). Presence/absence, differential expression and sequence polymorphisms between PiAVR2 and PiAVR2-like in *Phytophthora infestans* determine virulence on R2 plants. New Phytol **191,** 10.1111/j.1469-8137.2011.03736.x.

Milne, I., Lindner, D., Bayer, M., Husmeier, D., McGuire, G., Marshall, D.F., and Wright, F. (2009). TOPALi v2: a rich graphical interface for evolutionary analyses of multiple alignments on HPC clusters and multi-core desktops. Bioinformatics **25,** 126-127.

Tang, W., Yuan, M., Wang, R., Yang, Y., Wang, C., Oses-Prieto, J.A., Kim, T.W., Zhou, H.W., Deng, Z., Gampala, S.S., et al. (2011). PP2A activates brassinosteroid-responsive gene expression and plant growth by dephosphorylating BZR1. Nature cell biology **13,** 124-131.